SGP-TR-113-33

PROCEEDINGS
THIRTEENTH WORKSHOP
GEOTHERMAL RESERVOIR ENGINEERING

January 19-21, 1988

Henry J. Ramey, Jr., Paul Kruger, Frank G. Miller,
Roland N. Horne, William E. Brigham,
Jean W. Cook
Stanford Geothermal Program
Workshop Report SGP-TR-113*

*Sponsored by the Geothermal Technology Division of the U.S. Department of Energy, Stanford-DOE Contract No. DE-AS07-84ID12529

DISCLAIMER

PROCEEDINGS, Thirteenth Workshop on Geothermal Reservoir Engineering
Stanford University, Stanford, California, January 19-21, 1988
SGP-TR-113

Locating Hydraulically Active Fracture Planes

Mark Malzahn*, Donald Dreesen, and Michael Fehler

Los Alamos National Laboratory, Los Alamos, New Mexico 87545
*Contractor

ABSTRACT

If analysis of the microseismicity accompanying fluid injections is to be of maximum use in predicting hot dry rock (HDR) reservoir performance, it should lead to the determination of both the rock volume and active flowing surface area of the reservoir. In the granitic rock at the HDR geothermal site at Fenton Hill, New Mexico, the microearthquakes located during hydraulic fracturing occur in large three-dimensional volumes called seismic clouds. Cores cut from the region prior to fracturing show numerous planar fractures, some mineral-filled, at virtually random orientations. Evidence supports the hypothesis that only a few of these planes make up the flow path between wells for most of the injected fluid. If this is indeed the case, then it is necessary to be able to distinguish between fractures that accept flow from those which do not. We accomplish this by defining "flow-probable" planes to be those which have seismicity located relatively farther away from lines where other planes intersect. We show that these flow probable planes intercept wellbores at locations where other data confirm the presence of hydraulically active fractures.

INTRODUCTION

The location of planar features in large "clouds" of seismic events is accomplished by a new technique called the three point method (Fehler et al., 1987). Dreesen et al. (1987) showed correlations between well log anomalies (i.e. breakout zones, temperature depressions) and the plane/wellbore intercepts determined by the method. However, not all of the planes discovered by the three point method correlated with well log anomalies. This is because the method cannot distinguish among the following types of features:

1) Hydraulic features, including hydraulically-opened joints and hydraulically-fractured rock;
2) Structural features, including joints or faults, which contribute to fluid loss from the hydraulic features but which do not develop into significant flow paths;
3) Statistical features with no physical significance which result from a large number of microearthquakes coincidentally occurring along a plane.

We will describe the process used to determine whether or not a plane defined by the three-point method is likely to be a hydraulic feature. It does not deal with the distinction between structural and statistical features. Unless the structural features significantly affect the flowing portion of the reservoir, neither of these low-permeability features make much difference when it comes to reservoir modeling or selecting drilling targets for HDR reservoir creation.

IDENTIFICATION OF THE PLANES

The three point method was applied to a dataset consisting of 844 microseismic locations accompanying Experiment 2032 (Dreesen and Nicholson, 1985), a 21,200 m^3 injection which created a 42×10^6 m^3 seismic cloud (House et al., 1985); this resulted in the identification of 10 planar orientations. One feature of the method allows the extraction of the planes to occur in order of declining statistical significance (Fehler et al., 1987). Thus, the first orientation discovered is more likely to be an actual feature than the second, the second more likely than the third, etc. The first five planes all passed a statistical significance test that there be less than a 1 in 10,000 probability of being identified by chance. All 10 orientations were numbered in the order in which they were discovered. In addition, if analysis of the seismic data indicated the presence of two or more independent planes along the same orientation, each of these was labeled alphabetically. Table 1 lists the 21 planes, including strike and dip, associated with the ten most statistically significant orientations extracted from the Experiment 2032 dataset.

DESCRIPTION OF PLANES

The relative uncertainty between any two microseismic locations is roughly 20 meters (House, 1987). Thus, after locating the

planes, a search of the seismic data was conducted which assigned any seismic event occurring within 10 meters of either side of a plane to that plane. As a conservative measure, the 20 meter error was carried through to the spatial location of the planes, although the actual error is certainly much less since many events are used to define each plane.

The projection of all the events within 10 meters of either side of a plane onto that plane generates a unique pattern of seismicity upon each plane called the seismically active area; an example is shown in Figure 1. The seismically active areas are inferred to be the main regions of fluid flow in the planes, since the effective stresses in these areas have changed enough to cause slip to occur. This change in stress is attributed to the effects of pore fluid pressure (Fehler, 1987). The extent of a zone of weakness beyond the seismically active region of a plane is uncertain. However, it is possible that such a zone extends beyond the seismically active portion into the aseismic area, but that microearthquakes did not occur in these regions because of variations in the mechanical properties of the rock, or because the fluid that penetrated beyond the seismically active region was at insufficient pressure to induce seismicity.

The lines where all the other planes intersect a particular plane were also plotted. Two examples of the resulting images are given in Figure 2, which shows orthogonal views of the seismicity defining Plane 1A and Plane 2 along with the lines where other planes intersect these planes. These two planes are used to illustrate the difference between what we define as flow-probable and flow-improbable features.

A plane which is defined as flow-probable is one which has a relatively greater amount of seismicity occurring at a greater distance from lines where other planes intersect it, since such seismicity is more probably associated with only that plane. On Plane 2, virtually all seismicity occurs within 20 meters of a line of planar interception, as opposed to Plane 1A, upon which more than 25% of the seismicity occurs more than 20 meters away from any line of intersection. If a plane has a high percentage of its seismicity occurring near lines of planar interception, such as Plane 2, there is no way of knowing whether the plane is a true hydraulic feature, or is defined simply because of a large conflux of seismicity generated by hydraulic planes.

For each plane found from the Experiment 2032 dataset, Figure 3 shows the cumulative percentage of seismic events associated with a plane as a function of distance from the closest line of planar interception. These are separated into two groups according to their chances of being flowing features, probable or improbable. A flow-probable plane is defined as one having at least 25% of its seismicity occurring at least 15 meters away from any line of planar interception. The flow-improbable group is made up of the remaining planes.

RESULTS

By the above definition, planes 1A, 1B, 4A, 8A, 8B, and 10B make up the group of flow-probables, while the flow-improbable group consists of all the remaining planes. The depths were calculated where all the planes are projected to intercept the three wellbores, EE-2, EE-2A, and EE-3A, as were the minimum and maximum depths where the planes might intercept given the 20 meter error; this information is shown in Table 2. In some cases, as where Plane 1A intercepts EE-3A, there is no projected intercept, but there is a range along the well where an intercept may occur due to the 20 m error.

Temperature logs were then analyzed, superimposing the ranges of intercept depths for all the flow-probable planes along each log, in order to correlate thermal anomalies with the intercept points of these planes. The locations of anomalies, or departures from a constant thermal gradient, indicate either the production or injection of fluids along the well (Murphy, 1982).

Figure 4 shows that the interceptions of EE-2 by flow-probable planes 1A, 1B, and 10B correlate well with the locations of thermal anomalies in a log run on 7/27/82. The temperature log in Figure 4 was made following a smaller stimulation conducted prior to Experiment 2032. Therefore, the correlation of the planes discovered in the 2032 injection data with these anomalies supports the assumption that the flow paths are pre-existing features which are reopened each time the reservoir is pressurized.

Figure 5 shows two temperature logs run in well EE-3A, both taken after Experiment 2032. The log dated 7/10/85 followed a three-day injection into the interval from 3827 m to 4017 m. The two anomalies at 3150 m lie within the error band of flow-probable Plane 1A's location along the well, indicating that this plane might be actively cooling the liner even though it is quite a distance from the injection zone. This may also be the case at 3580 m, where two flow-probable planes, 4A and 8B, correlate with a thermal anomaly. The only flow-probable plane which intercepts the well in the injection interval is Plane 10B, which could be used to explain one of four anomalies.

The log dated 6/23/86 followed a month-long injection into an open-hole interval from 3487 m to 3750 m, and shows a myriad of temperature anomalies occurring both above and throughout the experimental injection zone. The temperature anomalies which are observed above the injection zone indicate flow due to the pressure gradient between the high-pressure injection zone and the low-pressure annular region 200 m above. Even though cement had effectively sealed the annulus, fluid was still able to flow away from the injection zone and cool the outer

casing through the damaged, more permeable rock immediately surrounding the cement. It is interesting to note, however, that most of these anomalies can be correlated with plane intercepts, and that two of the anomalies occur almost exactly where the flow-probable planes 8A and 1B are predicted to intercept the wellbore. If these are indeed flowing planes, then it is logical to assume that they would accept fluid in the region near their points of interception along the wellbore.

The log of the injection region for this experiment shows two minor and three major anomalies. The two minor anomalies, at 3490 m and 3510 m, correlate with the locations of flow-improbable planes 6 and 7B, implicating these planes as possible flowing features. However, the first minor anomaly occurs at precisely the top of the injection interval, and might be more simply explained by the aforementioned transition from cased to open hole. Also, both of these anomalies lie within the error band of flow-probable Plane 1B.

The first major anomaly, at 3550 m, lies within the range of flow-probable Plane 4A, and the second (3600 m) is within the range of both 4A and flow-probable Plane 8B. The last major anomaly at 3650 m does not correlate with any of the planes in this dataset. However, a more thorough examination of the data has shown a planar intersection in this region and is being investigated.

Figure 6 is a temperature log taken on 11/15/87 in the newly drilled well EE-2A during its first production test, showing several clear production points and two minor anomalies. Flow-probable Plane 10B correlates well with the anomaly at 3620 m. Flow-probable Plane 1B can explain the main anomaly at 3660 m or either of the rather less dramatic anomalies at 3670 m and 3680 m, or even the anomaly at 3620 m previously credited to Plane 10B. Flow-probable Plane 8B can also be correlated with the last anomaly at 3680 m. Of the remaining anomalies observed on this log, only the very small one at 3380 m can be correlated with any of the flow-improbable planes; in this case, it is Plane 6, another indication that this may be a flowing plane.

CONCLUSIONS

It has been hypothesized that a seismically active plane is more likely to be a flowing feature when a relatively greater amount of the seismicity by which it is defined lies at a greater distance from the lines of intersection formed by the remaining planes. As a test, a number of planes which were found in a set of microseismic data were classified as flow-probable or flow-improbable according to this hypothesis. We found that all of the planes defined as flow-probable showed a definite correlation with fluid injection or production points as defined by downhole temperature logs. While we could not correlate every temperature anomaly with a flow-probable plane, we could correlate every flow-probable plane with an anomaly. One obvious reason for a flow-probable plane not to show a correlation with a thermal anomaly is that the planes might only be flowing in their seismically active regions, while the wellbore may not intercept this region. While this method does not predict every injection or production point along a well, it can help increase the chances of encountering a flowing feature when confronted with a large choice of potential targets.

ACKNOWLEDGEMENT

We would like to thank Cheryl Straub, Bonita Busse, and Ruth Robichaud for their help with manuscript preparation. This work was supported by the U.S. Department of Energy, Geothermal Technology Division.

REFERENCES

Dreesen, D.S., Malzahn, M.V., Fehler, M.C., and Dash, Z.V. (1987), "Identification of MHF Fracture Planes and Flow Paths: A Correlation of Well Log Data with Patterns in Locations of Induced Seismicity," Geothermal Resources Council Transactions, Vol. 11, pp. 339-348.

Dreesen, D.S. and Nicholson, R.W. (1985), "Well Completion and Operations for MHF of Fenton Hill HDR Well EE-2," Geothermal Resources Council Transactions, Vol. 9, part II, p. 89.

Fehler, M. (1987), "Stress Control of Seismicity Patterns Observed During Hydraulic Fracturing Experiments Carried Out at the Fenton Hill Hot Dry Rock Geothermal Energy Site," Conference on Forced Fluid Flow in Fractured Rock Masses held in Garchy, France, (Proc. published by European Economic Commission in Brussels, Belgium).

Fehler, M., House, L. and Kaieda, H. (1987), "Determining Planes Along Which Earthquakes Occur: Method and Application to Earthquakes Accompanying Hydraulic Fracturing," Journal of Geophysical Research, Vol. 92, pp. 9407-9414.

House, L. (1987), "Locating Microearthquakes Induced by Hydraulic Fracturing in Crystalline Rock," Geophys. Rev. Letters, Vol. 14, pp. 919-921.

House, L., Keppler, H., and Kaieda, H. (1985), "Seismic Studies of a Massive Hydraulic Fracturing Experiment," Geothermal Resources Council Transactions, Vol. 9, part II, pp. 105-110.

Murphy, H.D. (1982), "Enhanced Interpretation of Temperature Surveys Taken During Injection or Production," Journal of Petroleum Technology, June, p. 1313.

TABLE 1

Strike and Dip of All Planes Associated with the 10 Most Likely Orientations Found in the Experiment 2032 Dataset
(all angles in degrees)

Plane	Strike	Dip
1A	N29W	76E
1B	N29W	76E
2	N88E	27W
3A	N29W	67W
3B	N29W	67W
4A	N6E	67E
4B	N5E	64E
4C	N8E	67E
5A	N33E	60W
5B	N34E	56E
6	N64W	67W
7A	N84E	32W
7B	N86E	33W
7C	N81E	36W
7D	N86E	34W
8A	N21W	58E
8B	N20W	61E
9A	N79W	74E
9B	N79W	74E
10A	N35W	82W
10B	N32W	81W

TABLE 2

Minimum, Projected, and Maximum Depths of Interception Along Each Wellbore for Each Plane
(all measurements in meters along wellbore)

Plane	Well EE-2			Well EE-3A			Well EE-2A		
	minimum	projected	maximum	minimum	projected	maximum	minimum	projected	maximum
1A	3587	3617	3647	3072	--	3186	3691	3759	3765
1B	3527	3557	3587	3205	3349	3417	3569	3627	3694
2	4093	4107	4122	3849	3860	3871	--	--	--
3A	3249	3263	3277	3140	3159	3177	3248	3262	3275
3B	3267	3281	3295	3162	3181	3199	3265	3279	3292
4A	3007 3759	3056 3848	3128 3934	3540	3574	3609	3005	3042	3081
4B	--	--	--	3663	3692	3722	3548	3641	3719
4C	--	--	--	3801	3839	3878	--	--	--
5A	3640	3657	3674	3518	3534	3550	3651	3667	3683
5B	4047	4061	4074	3926	3940	3954	--	--	--
6	3395	3410	3424	3459	3491	3522	3374	3389	3405
7A	2991	3004	3017	3020	3032	3044	2994	3008	3022
7B	3555	3573	3592	3478	3489	3500	3554	3569	3584
7C	3657	3677	3696	3531	3542	3554	3637	3652	3667
7D	4215	4231	4247	3891	3902	3913	--	--	--
8A	3192 4208	3234 4508	3288 4660	3430	3451	3470	3185	3239	3310
8B	--	--	--	3559	3582	3605	3674	3755	3764
9A	--	--	--	--	--	--	--	--	--
9B	--	--	--	4008	--	4016	--	--	--
10A	3402	3419	3437	3296	3334	3380	3392	3410	3429
10B	3578	3593	3608	3906	3955	4001	3603	3622	3641

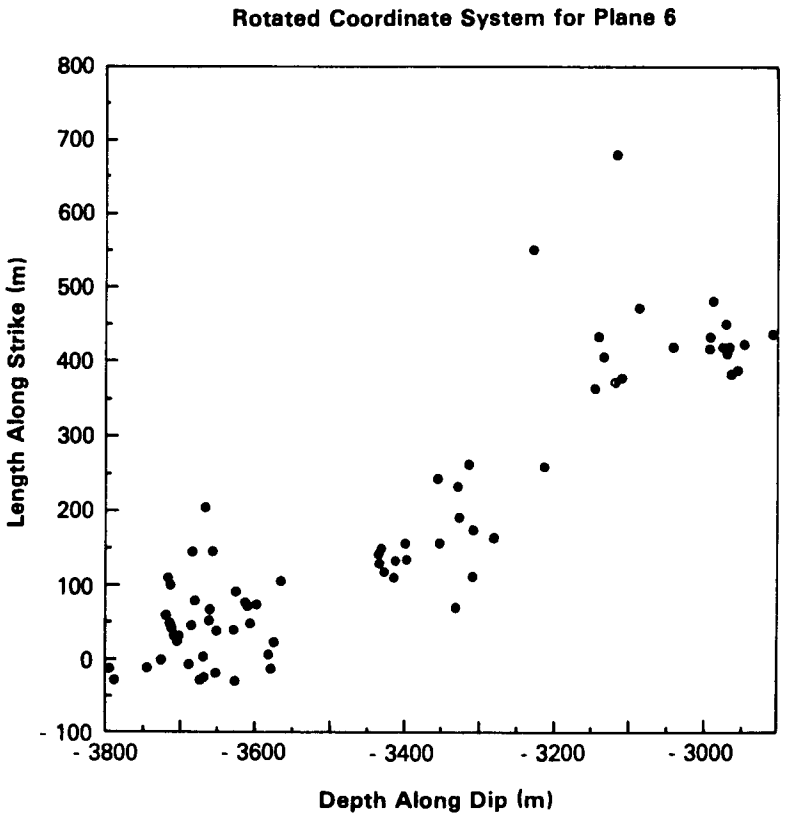

Figure 1: An orthogonal view of Plane 6. The dots mark the locations of all the seismic events associated with this plane, each of which lies within 10 m of either side of the plane.

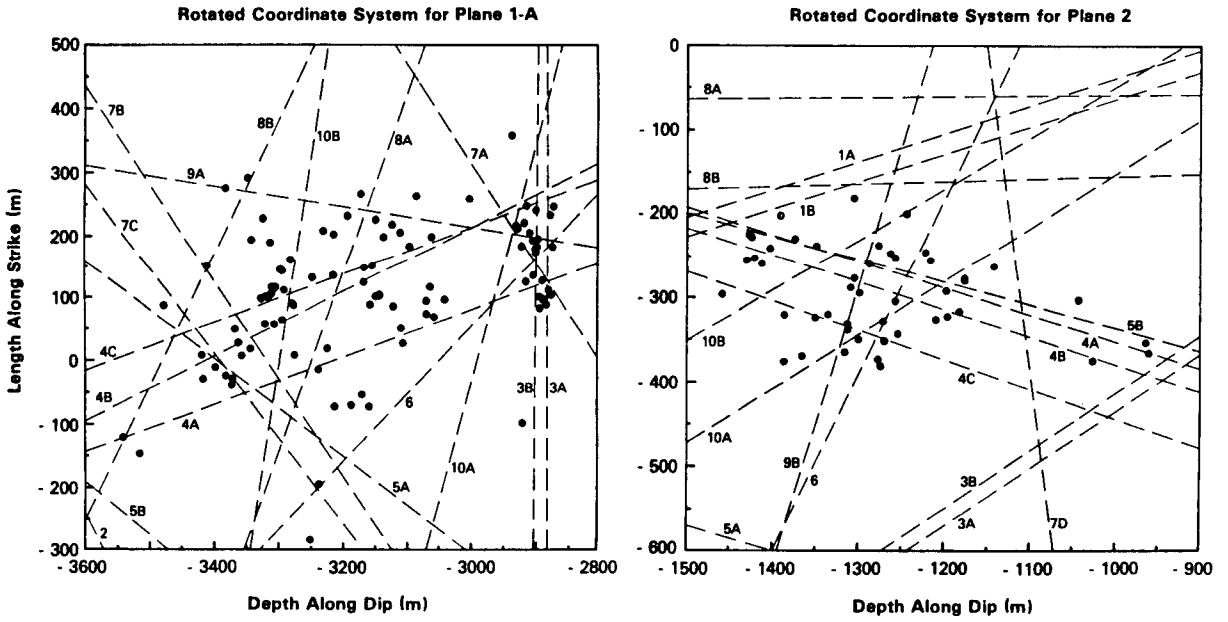

Figure 2: Orthogonal views of planes 1A and 2, including the seismic events which define each plane as well as the lines of intersection made by each of the remaining planes. The seismicity defining Plane 2 generally lies closer to a line of planar intersection than does the seismicity defining Plane 1A; thus, compared to each other, Plane 1A is flow-probable, and Plane 2 is flow-improbable.

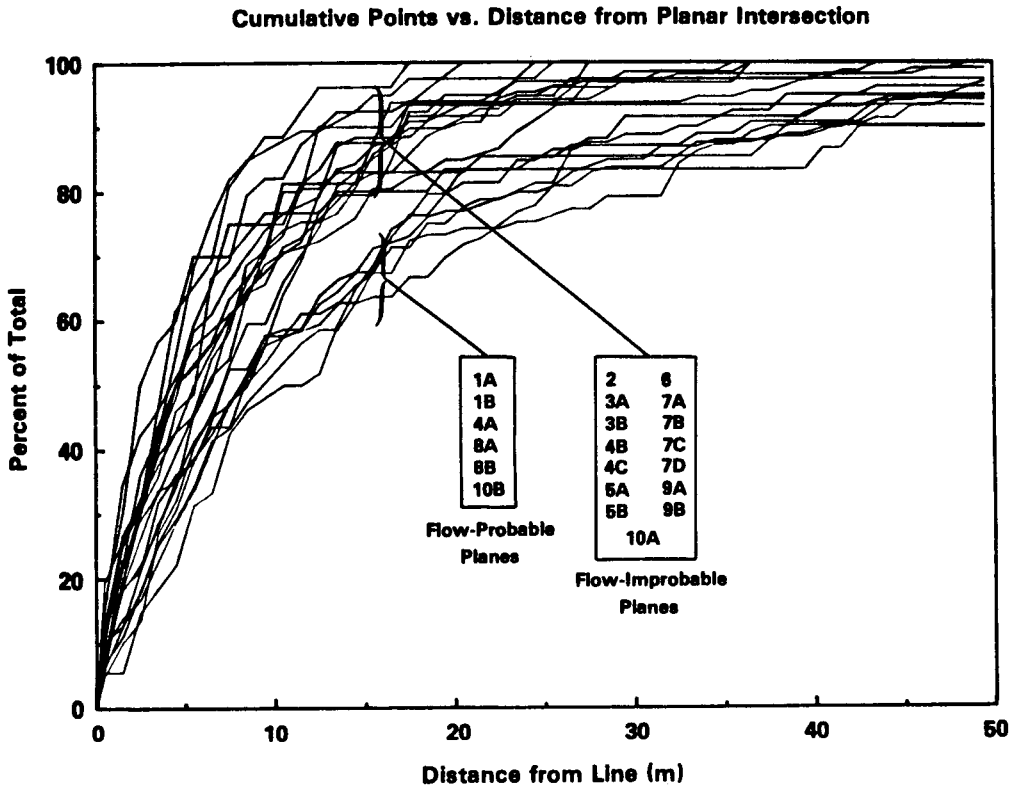

Figure 3: Percent of total seismicity as a function of distance from the nearest line of planar intersection for each plane. Flow-probable planes have at least 25% of their seismicity occurring at least 15 m away from any line of planar intersection.

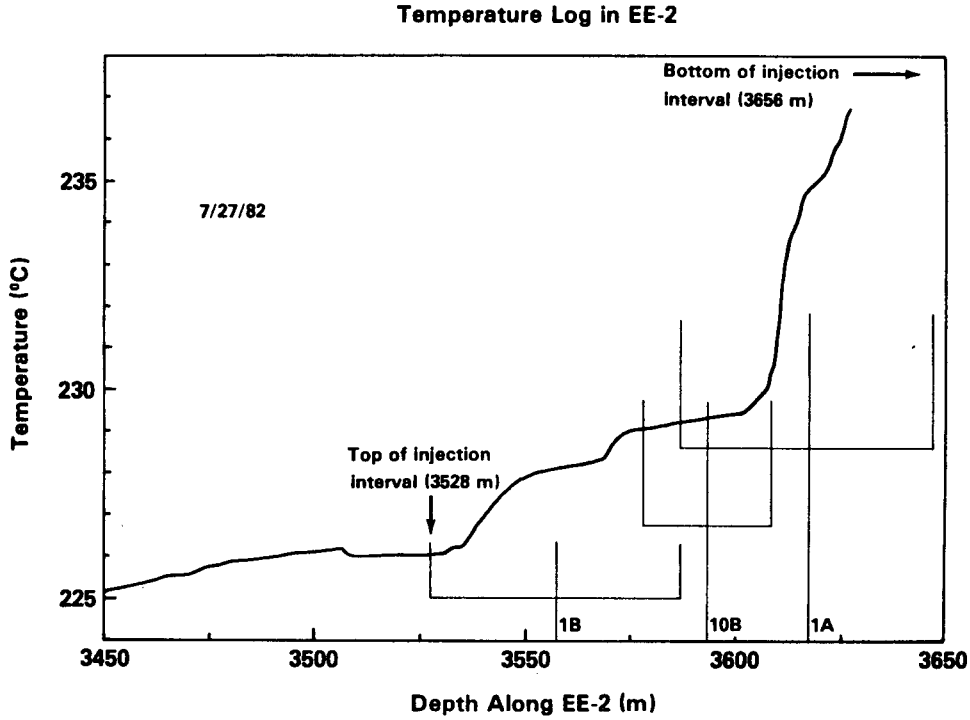

Figure 4: Correlation of thermal anomalies in EE-2 with flow-probable planes.

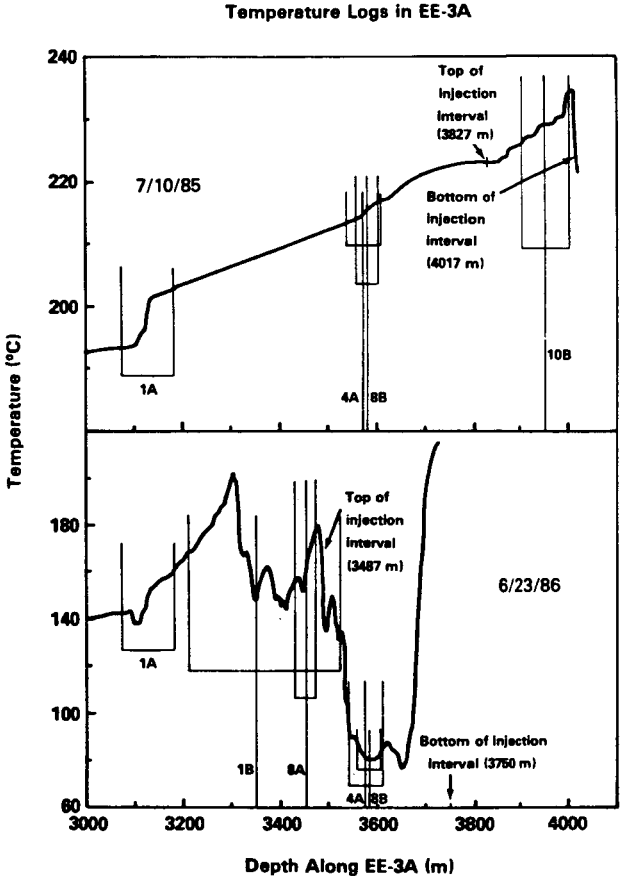

Figure 5: Correlation of thermal anomalies with flow-probable planes in two temperature logs run in EE-3A.

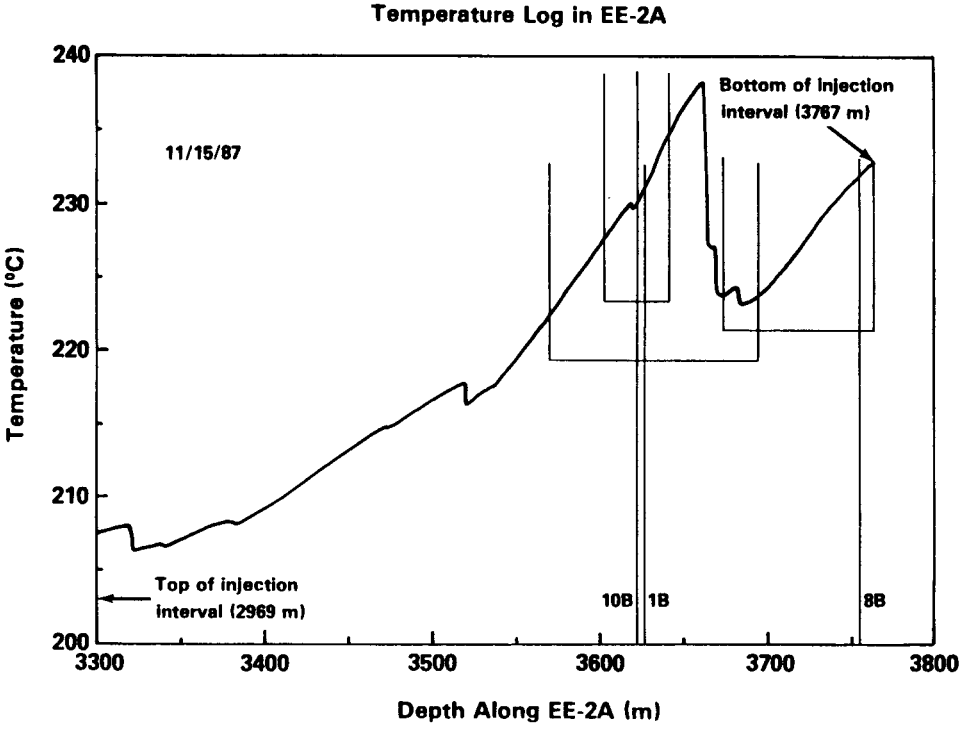

Figure 6: Correlation of thermal anomalies in EE-2A with flow-probable planes.